The Influence of Bone Type on the Gene Expression in Normal Bone and at the Bone-Implant Interface: Experiments in Animal Model

Omar Omar, BDS;* Felicia Suska, PhD;† Maria Lennerås, MSc;‡ Neven Zoric, MSc;§ Sara Svensson, MSc;¶ Jan Hall, MSc;** Lena Emanuelsson, BS;†† Ulf Nannmark, DDS, PhD;‡‡ Peter Thomsen, MD, PhD§§

ABSTRACT

Background: Studies on the biological processes in different bone types and the reaction of different bone types to biomaterials are often hindered because of the difficulties in sampling procedures and lack of sensitive techniques.

Purpose: The purpose was to assess the suitability of quantitative polymerase chain reaction (qPCR) for investigation of the biological differences between cortical and trabecular bone types and their responses to biomaterials.

Materials and Methods: Gene expression of selected markers in rat bone samples from different locations was evaluated. Samples were harvested by trephines from the trabecular femoral epiphysis, cortico-trabecular proximal tibial metaphysic, and the cortical distal tibial metaphysis. Gene expression was also evaluated at the surfaces of anodically oxidized implants retrieved from cortical and trabecular sites after 3 days of implantation. mRNA in the bone samples and in the tissue associated with the implant surfaces was extracted and quantified using qPCR. Tumor necrosis factor-α (TNF-α), interleukin-1β (IL-1β), alkaline phosphatase (ALP), osteocalcin (OC), tartrate-resistant acid phosphatase (TRAP), cathepsin K (CATK), and 18S ribosomal subunits (18S) were analyzed.

Results: In the bone samples, higher expression of ALP, OC, TRAP, and CATK was found in femoral epiphysis compared to proximal or distal tibial metaphysis, indicating a higher turnover in the trabecular bone. On the other hand, TNF-α and IL-1β showed higher expression in both tibia sites compared with the femur site, which suggests higher inflammatory potential in the cortical bone. In response to the oxidized implants trabecular bone expressed a higher level of IL-1β, whereas the implants in cortical bone were associated with higher expression of ALP and OC.

Conclusion: There are biological differences between cortical and trabecular bone types, both in the normal steady-state condition and in response to biomaterials. Such differences can be characterized and discriminated quantitatively using a sensitive technique such as qPCR.

KEY WORDS: cortical bone, gene expression, in vivo, titanium implants, trabecular bone

INTRODUCTION

The basic architecture of bone is divided into two types: cortical and trabecular. The two types are distributed at different anatomical locations in the body skeleton. They differ not only in the tissue macro-architecture,

*PhD student, Department of Biomaterials, Sahlgrenska Academy at University of Göteborg, Sweden; †Department of Biomaterials, Sahlgrenska Academy at University of Göteborg, Sweden; ‡research scientist, TATAA Biocenter AB, Göteborg, Sweden; §general manager, TATAA Biocenter AB, Göteborg, Sweden; ¶PhD student, Department of Biomaterials, Sahlgrenska Academy at University of Göteborg, Sweden; **chief scientist, Nobel Biocare AB, Göteborg, Sweden; ††laboratory technician, Department of Biomaterials, Sahlgrenska Academy at University of Göteborg, Sweden; ‡‡associate professor, Department of Medical Biochemistry and Cell Biology, Institute of Biomedicine, Göteborg, Sweden; §§professor, Department of Biomaterials, Sahlgrenska Academy at University of Göteborg, Sweden; scientific leader, Institute of Biomaterials and Cell Therapy, Göteborg, Sweden; director, BIOMATCELL VINN Excellence Center of Biomaterials and Cell Therapy, Göteborg, Sweden

Reprint requests: PhD student, Omar Omar, Medicinaregatan 8B, 41390 Göteborg, Sweden; e-mail: omar.omar@biomaterials.gu.se

DOI 10.1111/j.1708-8208.2009.00195.x

but also in their cellular contents, metabolic rates, and bone marrow constituents. These structural and biological differences could probably result in different responses to injury and biomaterial insertion, and have different effects on the remodeling processes of the two bone types. To date, there are no studies exploring differences between cortical and trabecular bone types on the gene expression level.

The cellular and molecular activities governing the early inflammatory responses and subsequently the tissue repair and remodeling in close vicinity to the implant in different bone types are yet to be described. Haider and colleagues[1] demonstrated that spongy bone reacts with more and earlier new bone formation to titanium implants compared to compact bone. Davies[2] claimed that trabecular bone represents a biologically superior tissue, ideally evolved for rapid (peri-implant) bone healing, when compared to the slowly remodeling healing pattern typical of cortical bone. Histomorphological evaluations of biomaterials with different properties, including free-form fabricated porous hydroxyapatite (HA) scaffolds[3] and HA-coated titanium implants,[4] showed trabecular bone to have an advantageous response to such biomaterials. To our knowledge there is no study describing the difference in gene expression between the two bone types in their responses to titanium implants. We have recently developed an in vivo model for studies on early gene expression in cells adherent to implants.[5] This model may be a useful method to identify differences between different tissues in their responses to biomaterials and, in addition, it may provide detailed understanding of the biological and molecular basis of the osseointegration.

Many techniques have been used to analyze the cellular and molecular activities in undecalcified and decalcified bone tissues. At the protein level, immunohistochemistry, Enzyme-Linked Immunosorbent Assay, and Western blot[6–11] are the most commonly used techniques. At the gene expression level, microarray analysis, in situ hybridization, and semiquantitative reverse transcription polymerase chain reaction (RT-PCR) techniques have been used.[12–18] qPCR represents a promising new tool to spatially and temporally analyze biological processes in bone with a high level of precision and accuracy. qPCR has been used in many in vitro studies analyzing the interactions between bone cells and biomaterial surfaces.[19–21] However, few in vivo studies[5,22–24] are available and detailed studies on bone types and normalization methods have not been reported.

The aims of this study were twofold. First, to apply qPCR for determining the differences in gene expression denoting inflammation and bone remodeling between bone samples with different cortical and trabecular constituents. Second, to determine if the gene expression is influenced by the presence of a biomaterial and how then the cortical and trabecular bone respond to titanium implants at an early time point. The study addressed the expression of selected markers of inflammation (tumor necrosis factor-alpha [TNF-α] and interleukin-1beta [IL-1β]), bone formation (osteocalcin [OC] and alkaline phosphatase [ALP]), and bone resorption (tartrate-resistant acid phosphatase [TRAP] and cathepsin K [CATK]). The effect of the sample weight on the levels of gene expression was also assessed.

MATERIALS AND METHODS

Implants

Anodically oxidized screw-shaped titanium implants (TiUnite™; Nobel Biocare, Göteborg, Sweden), 2 mm in diameter and 2.3 mm in length, were used. The surface roughness (Ra) is 1.2 μm, as measured by light interferometry (MicroXAM Interferometric Profiler, ADE Phase Shift, Tucson, AZ, USA). The test implants were manufactured and sterilized by Nobel Biocare.

Surgical Procedure

The animal experiment was approved by the local ethical committee for laboratory animals (306-2006). A total of thirty adult female Spraque–Dawley rats (200–250 g), fed on a standard pellet diet and water were used for the study. The rats were divided into three groups: 18 rats were used for analyzing the gene expression at the implant surface; eight rats for studying steady-state gene expression in bone biopsies; and four rats for histology. The first group of rats were anesthetized using a Univentor 400 anesthesia unit (Univentor Ltd., Zejtun, Malta) under isoflurane (Isoba® Vet, Schering-Plough Ltd. Uxbridge, England) inhalation. Anesthesia was maintained by continuous administration of isoflurane via a mask. Each rat received analgesic (Temgesic 0.03 mg/kg, Reckitt & Coleman, Hull, Great Britain) subcutaneously prior to the implantation and daily postoperatively. After shaving and cleaning, the medial aspect of either distal femoral epiphysis or tibial metaphysis was exposed. After soft tissue reflection, the bone was

prepared with Ø1.4 and Ø1.8-mm burs under profuse irrigation with 0.9% NaCl. The implants were installed in the distal femoral epiphysis of nine rats and the distal tibial metaphysis of another nine rats ($n = 9$). The wounds were sutured and the animals were allowed free postoperative movements with food and water ad libitum. The retrieval procedure was performed after 3 days. The rats were sacrificed by an intraperitoneal overdose of sodium pentobarbital (60 mg/mL; ATL Apoteket Production & Laboratories, Kungens Kurva, Sweden) under anesthesia with a 0.5-mL mixture of pentobarbital (60 mg/mL), sodium chloride, and diazepam (1:1:2), and cleaned with 5 mg/mL chlorohexidine in 70% ethanol. Because of the early retrieval time point, the implants were not yet strongly integrated in bone, and could therefore be unscrewed with adherent biological material by a hexagonal screw driver. The implants were immediately placed in preserving solution (RNA*later*®, QIAGEN GmbH, Hilden, Germany). The eight rats of the second group were sacrificed as described earlier. Bone samples from femoral epiphysis, proximal, and distal tibial metaphysis of both legs were retrieved using two different size trephines with diameters of 2.1 and 2.3 mm. The samples were immediately placed in preweighed RNA*later*® containing tubes, and the wet weight (in grams) of each sample was registered. The retrieval procedure of the bone samples and the implants was performed according to an RNA-preserving protocol established by the research group. In brief, the surgical procedure was performed with restrict precaution (RNase-free saline was used for irrigation and RNase-free tubes were used to collect the qPCR samples). The RNA was maintained for 7 days in a fridge at 4°C and then stored at −80°C until analysis.

Histology

The third group of four rats was used for histology. Two rats received oxidized titanium implants in the femoral epiphysis and the distal tibial metaphysis of both legs ($n = 2$) and sacrificed after 3 days as described earlier. The bone-implant specimens were dissected and fixated in formaldehyde. Specimens were decalcified in 10% ethylenediaminetetraacetic acid for 10 to 12 days. The specimens were then dehydrated in ascending series of ethanol, cleared with xylene, and embedded in paraffin. As the paraffin was still in melting stage, the implants were unscrewed and the embedding procedure was continued. The idea behind removing the implant at this stage was to preserve the implant-bone interface as intact as possible. Subsequently, 10-µm sections (bone-implant sections) were produced, mounted on glass slides, and stained with hematoxylin and eosin (H&E) for light microscopic observationrats. The other two rats were sacrificed as described earlier and bone specimens from distal femoral epiphysis and tibial metaphysis were harvested. The bone specimens were prepared for either H&E-stained decalcified paraffin embedded or toluidine blue-stained ground sections (bone sections).

Quantitative PCR

The bone samples and the unscrewed implants were placed in RNA*later*® solution (QIAGEN GmbH) and stored at −80°C until analysis. The bone samples were homogenized in phenol/guanidine-based Qiazol lysis reagent using 5-mm stainless steel beads (QIAGEN GmbH) and TissueLyser (QIAGEN GmbH). After the addition of chloroform, the samples were centrifuged at 12,000 *g* for 15 minutes, and the aqueous phase was used for subsequent RNA extraction. Total RNA from the bone samples and from the implants was extracted using RNeasy® Mini kit and Micro kit (QIAGEN GmbH), respectively, according to the manufacturer's instructions. DNAse treatment was performed in order to eliminate any contamination from genomic DNA. Reverse transcription was carried out using iScript cDNA Synthesis Kit (Bio-Rad, Hercules, CA, USA) in a 10-µL reaction, according to the manufacturer's instructions. Design of primers for ALP, OC, TRAP, CATK, TNF-α, IL-1β, and 18S was performed using the Primer3 web-based software.[25] Assays were purchased from TATAA Biocenter AB, Göteborg, Sweden. Design parameters were adjusted to minimize formation of artifact products and to allow for an annealing temperature in the PCR at about 60°C. Primers were designed to yield short amplicons (preferably shorter than 200 bp) and to function well with SYBR Green I fluorescent dye for detection of the PCR products in real-time. qPCR was performed in duplicates using the Mastercycler ep realplex (Eppendorf, Hamburg, Germany) in 20-µL reactions. Cycling conditions were 95°C for 10 minutes followed by 45 cycles of 95°C for 20 s, 60°C for 20 s, and 72°C for 20 s. The fluorescence was read at the end of the 72°C step. Melting curves were recorded after the run by stepwise temperature increase (1°C/5 s) from 65 to 95°C. The quantities of target genes were normalized using the expression of 18S. The normalized relative

quantities were calculated using the delta Ct method and 90% PCR efficiency ($k^*1.9^{\Delta ct}$).[26]

Statistics

For comparison of gene expression at different bone sites, one-way analysis of variance was used ($n = 15$ for each bone type) followed by multiple comparison Fisher protected least significant difference test to compare pairs of means (SPSS® version 15.0, SPSS Inc., Chicago, IL, USA). Mann-Whitney test was used to analyze differences in the gene expression levels between the implants in the two compared locations (i.e., femur and tibia) ($n = 9$). The level of confidence for either test was set to 95%, that is, $p < 0.05$ was significant. The data presented in the graphs is mean ± standard error of the mean.

For determination of the correlation between bone sample weight and 18S expression; linear regression analysis (SPSS® version 15.0) was conducted using the sample weight in gram as the independent variable and the 18S expression as the dependent variable.

RESULTS

Gene Expression Analysis

The panel of gene markers was divided into three groups: bone formation; bone resorption; and pro-inflammatory markers. First, the expression of this panel of genes was evaluated in bone samples from femur, proximal tibial metaphysic, and distal tibial metaphysis representing trabecular, mixed cortico-trabecular, and mainly cortical bone types respectively. Then, the panel of genes was measured and compared in cells adherent to the anodically oxidized titanium implants after unscrewing them from either trabecular or cortical bone locations. The data are presented as total (Figure 1A, Table 1) and 18S-normalized gene expression (Table 2; see also Figure 1B). The gene expression levels at implants retrieved from different bone types were compared based on the normalized data only (Figure 2A).

18S Ribosomal RNA Expression. The expression of 18S ribosomal RNA is indicative for the total cell number in the bone samples or the total number of cells adherent to the implant surface. The results from the bone samples showed higher levels of 18S in the proximal mixed bone of the tibia compared to the femoral trabecular bone (see Figure 1C and Table 1). No significant difference was observed in the expression of 18S between the implants retrieved from the femoral trabecular bone and the distal tibial cortical bone (see Figure 2B).

Expression of Bone Formation Markers (ALP and OC). The total ALP expression was significantly higher, by a factor of 2 and 2.6, in the femur compared with the proximal and distal tibia, respectively (see Figure 1A and Table 1). A similar pattern was observed for the 18S-normalized ALP expression with threefold higher expression in the femur compared with the proximal and distal tibia (see Figure 1B and Table 2). For OC, the total expression was twofold higher in the femoral and proximal tibial bone compared with the distal tibial bone (see Figure 1A and Table 1). The normalized OC expression was significantly higher, by a factor of 2, in the femur compared with the distal tibia (see Figure 1B and Table 2).

The normalized expression levels of ALP and OC were 12- and 41-fold, respectively, higher at the implants retrieved from the tibial cortical bone than those retrieved from the femoral trabecular bone (see Figure 2A).

Expression of Bone Resorption Markers (TRAP and CATK). The femoral total expression of TRAP was threefold higher compared to the proximal tibia and 11-fold higher compared with the distal tibia (see Figure 1A and Table 1). The normalized TRAP expression level was fivefold higher in the femur compared with the proximal tibia (see Figure 1B and Table 2). The total CATK expression was higher by a factor of 10 in the femoral spongisa compared with the distal tibial compacta. Similarly, the mixed cortico-trabecular proximal tibia showed a higher total expression of CATK (10-fold) compared with the cortical distal tibia (see Figure 1A and Table 1). No significant differences in the normalized expression of CATK were observed among the different bone sites.

No significant differences could be observed between the two locations when comparing the expression levels of the bone resorption markers at the implants retrieved from the femur and tibia (see Figure 2A).

Expression of Pro-Inflammatory Markers (TNF-α and IL-1β). The total and 18S-normalized expression levels of TNF-α and IL-1β had similar patterns and were

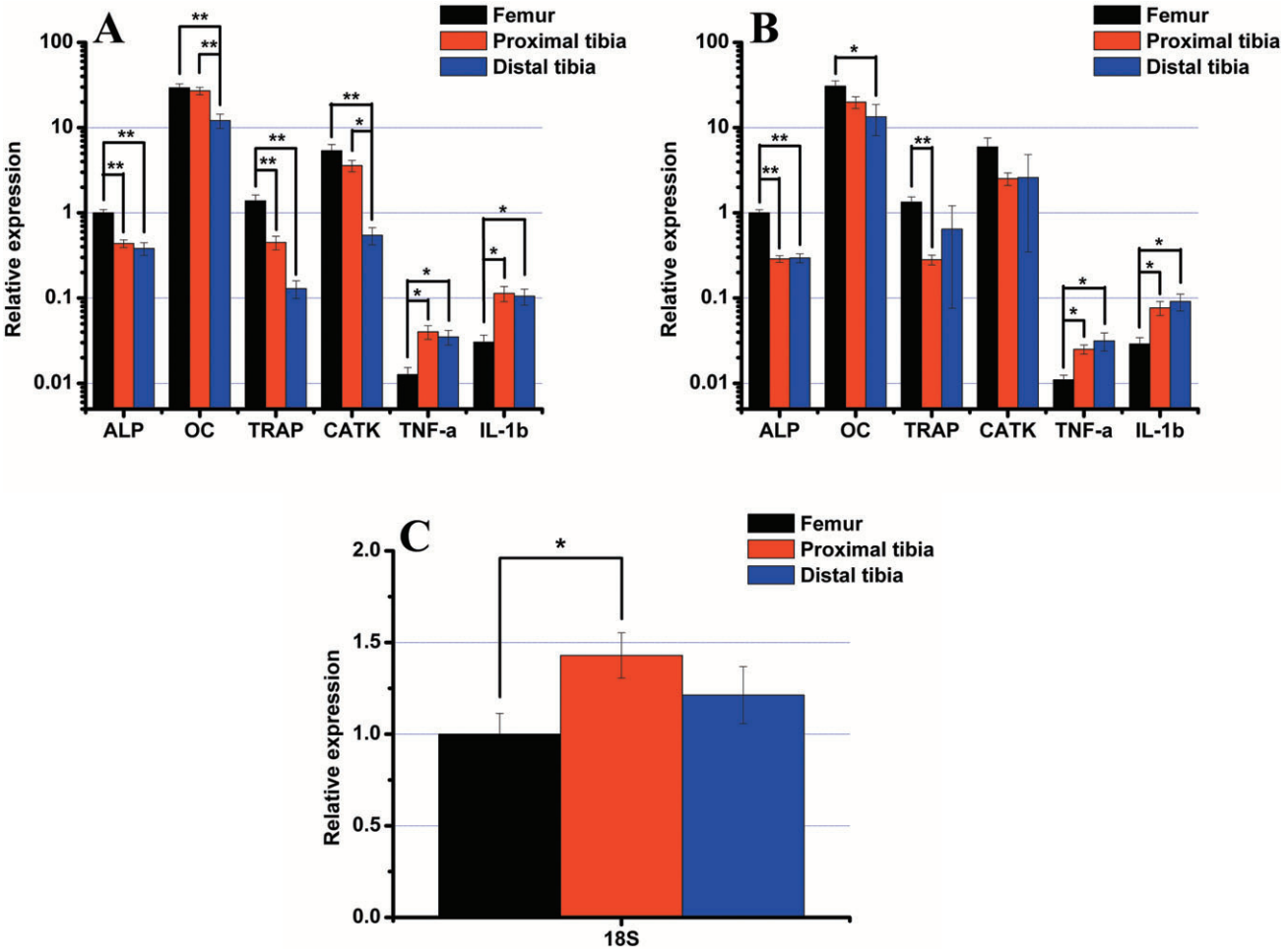

Figure 1 Gene expression in rat bone. The total (A) and 18S-normalized (B) relative expression levels of bone formation, bone resorption, and pro-inflammatory markers. *C*, The 18S ribosomal RNA expression. Statistically significant differences between the different bone types are indicated in stars (*$p < 0.05$; **$p < 0.005$) $n = 15$; mean ± standard error of the mean. 18S = 18S ribosomal subunits; ALP = alkaline phosphatase; OC = osteocalcin; TRAP = tartrate-resistant acid phosphatase; CATK = cathepsin K; TNF-α = tumor necrosis factor-α; IL-1β = interleukin-1β.

significantly higher in both proximal and distal tibia compared with the femur (see Figure 1, A and B, Tables 1 and 2).

A reversed pattern was seen with the implants. Anodically oxidized implants retrieved from trabecular femoral bone showed twofold higher expression of IL-1β compared with the similar implants retrieved from the tibial cortical bone (see Figure 2A).

Correlation Between Sample Wet Weight and Total Amount of 18S Gene Expression. The 18S mRNA expression levels were correlated to the wet weight (in grams) of the samples in order to find the most optimal way to normalize gene expression. Linear regression analysis did not show a linear correlation between the sample

TABLE 1 Ratio of Total RNA Expression Between Different Bone Types

	Femur[a]/ Proximal Tibia[b]	Femur[a]/ Distal Tibia[b]	Proximal Tibia[a]/ Distal Tibia[b]
18S	0.70*	0.82	1.18
ALP	2.29*	2.62**	1.15
OC	1.09	2.43*	2.24*
TRAP	3.08*	10.71**	3.48*
CATK	1.49	9.81**	6.57*
TNF-α	0.31*	0.36*	1.15
IL-1β	0.27*	0.29*	1.08

Results presented as the ratios among the total mRNA expression levels of different markers in femoral epiphysis, proximal tibial metaphysis, and distal tibial metaphysis ($n = 15$). Values more than 1 indicate more gene expression in [a] whereas values below 1 indicate more gene expression in [b]. Statistically significant differences between the different bone types are indicated in asterisks (*$p < 0.05$; **$p < 0.005$).
18S = 18S ribosomal subunits; ALP = alkaline phosphatase; OC = osteocalcin; TRAP = tartrate-resistant acid phosphatase; CATK = cathepsin K; TNF-α = tumor necrosis factor-α; IL-1β = interleukin-1β.

TABLE 2 Ratio of Normalized RNA Expression Between Different Bone Types

	Femur[a]/ Proximal Tibia[b]	Femur[a]/ Distal Tibia[b]	Proximal Tibia[a]/ Distal Tibia[b]
ALP	3.47**	3.38**	0.97
OC	1.54	2.29*	1.49
TRAP	4.75**	2.08	0.44
CATK	2.35	2.29	0.97
TNF-α	0.44*	0.35*	0.80
IL-1β	0.38*	0.32*	0.84

Results presented as the ratios among the 18S-normalized mRNA expression levels of different markers in femoral epiphysis, proximal tibial metaphysis, and distal tibial metaphysis ($n = 15$). Values more than 1 indicate more gene expression in [a] whereas values below 1 indicate more gene expression in [b]. Statistically significant differences between the different bone types are indicated in asterisks (*$p < 0.05$; **$p < 0.005$).
18S = 18S ribosomal subunits; ALP = alkaline phosphatase; OC = osteocalcin; TRAP = tartrate-resistant acid phosphatase; CATK = cathepsin K; TNF-α = tumor necrosis factor-α; IL-1β = interleukin-1β.

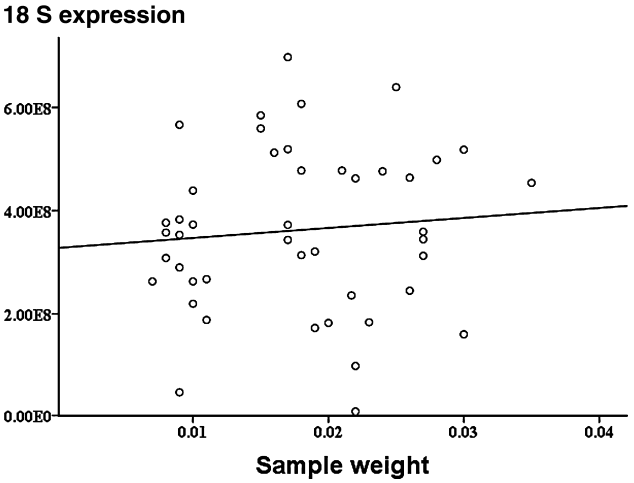

Figure 3 Correlation analysis between sample weight (in grams) and expression of 18S. The curve estimation indicated that no linear correlation exists between the sample weight and the total expression level of 18S (the indicative of total cell number present in the sample).

wet weight and the 18S expression (Figure 3). The R^2 was 0.008 and no linear correlation was apparent.

Histological Analysis

In the bone sections (decalcified or ground) the rat bone showed higher activity of coupled bone resorption and bone formation in the proximal tibia compared with the distal tibia (Figure 4, A–C). Large multinucleated osteoclasts were seen actively resorbing bone followed by osteoblast seams depositing new bone (see Figure 4B). The femur samples, retrieved 2 mm distal to the joint, represented predominantly trabecular bone (Figure 5A). The proximal tibial metaphysis samples, retrieved 2 mm distal to the joint, contained mixed cortical and trabecular bone whereas the distal tibial metaphysis samples, retrieved 5 mm distal to the joint, contained mainly cortical bone (see Figure 5B). Femoral epiphysis sections showed foci of active endochondral bone formation at some areas of the epiphysis (see Figure 4, D–F). These areas include growth plates with zones of column formation, chondrolysis, and

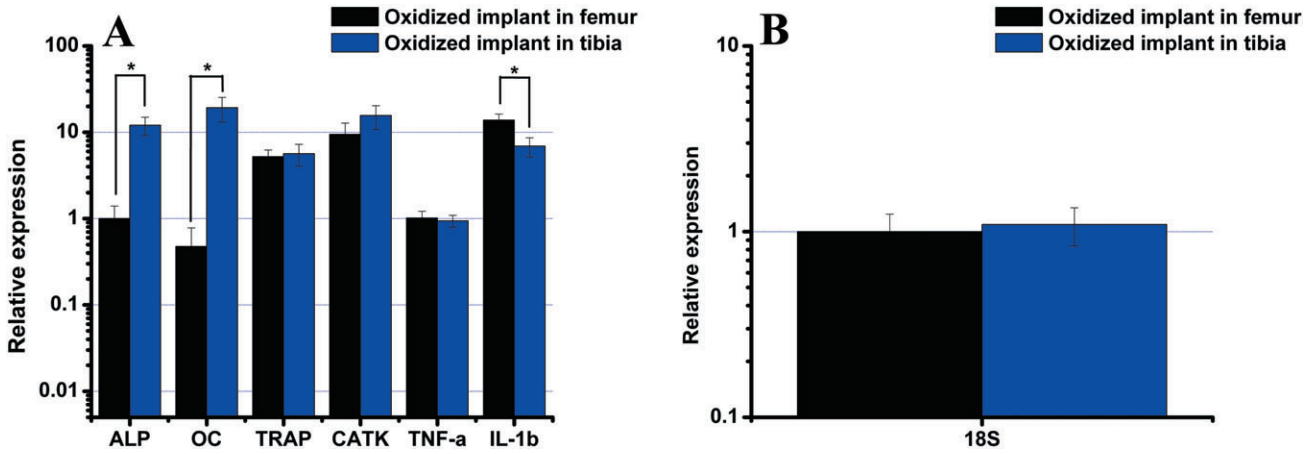

Figure 2 Gene expression at the oxidized implants in femur and tibia. *A*, 18S-normalized relative expression of bone formation, bone resorption, and pro-inflammatory markers. *B*, The 18S ribosomal RNA expression. Statistically significant differences at the implant surfaces in different bone types are indicated in stars (*$p < 0.05$; **$p < 0.005$) $n = 9$; mean ± standard error of the mean. 18S = 18S ribosomal subunits; ALP = alkaline phosphatase; OC = osteocalcin; TRAP = tartrate-resistant acid phosphatase; CATK = cathepsin K; TNF-α = tumor necrosis factor-α; IL-1β = interleukin-1β.

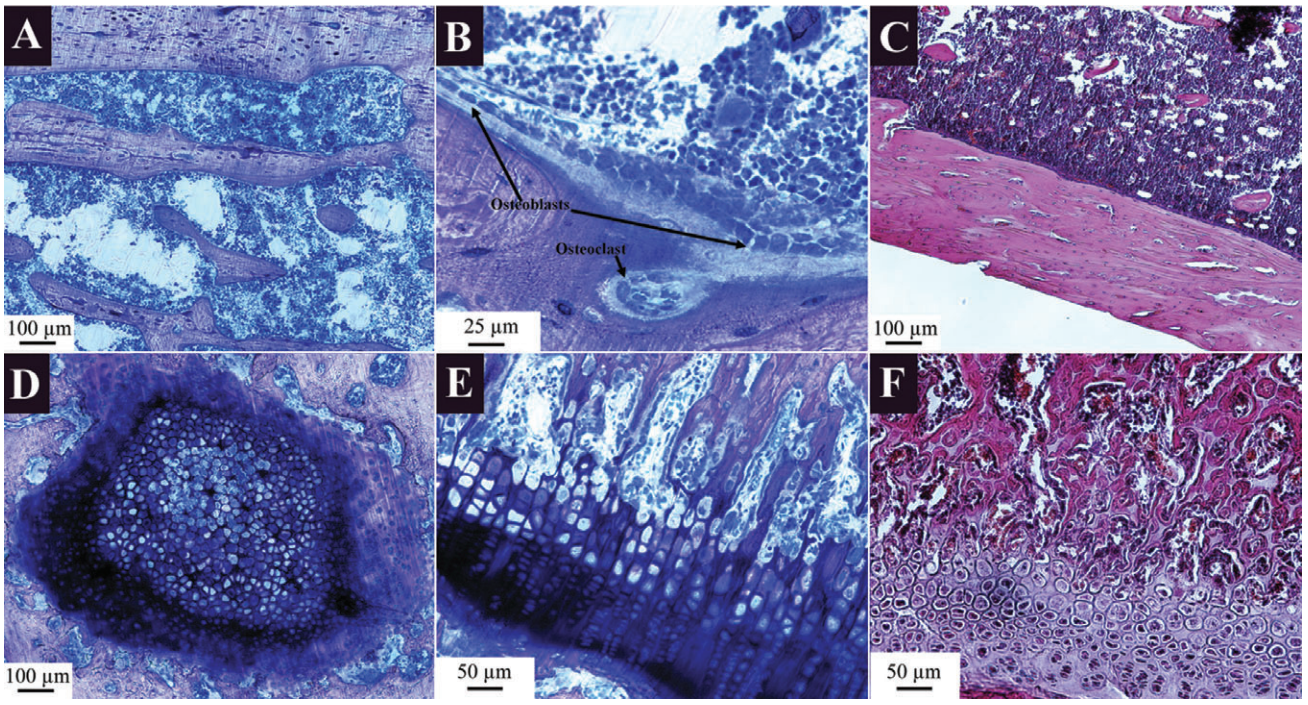

Figure 4 Histological ground and decalcified sections of rat tibia and femur. *A*, Ground section of proximal tibial metaphysis showing high amount of trabecular bone (magnification ×10). *B*, Higher magnification view of proximal tibial metaphysis showing active bone resorbing osteoclast followed by seam of osteoblast forming new bone (×40). *C*, Decalcified paraffin-embedded and H&E-stained section of distal tibial metaphysis in purely cortical form. Adjacent to the cortex is the bone marrow consisting of different cell populations with spaces of fat (×10). Ground cross- (D) and longitudinal- (E) sections of femur epiphysis showing foci of endochondral bone formation (×20 and ×40, respectively). *F*, Paraffin-embedded and H&E-stained longitudinal section of femur epiphysis showing active endochondral bone formation (×20). H&E = hematoxylin and eosin.

ossification. Actively mitotic zones of cells were also seen. The bone-implant sections shows that implants were well-positioned unicoritically in the cortical tibial bone and penetrating into the medullary canal (Figure 6A). An observation was that the implant-tissue interface from the tibial site was more intact after unscrewing the implants compared with the trabecular site. The tibial site showed a higher degree of new tissue

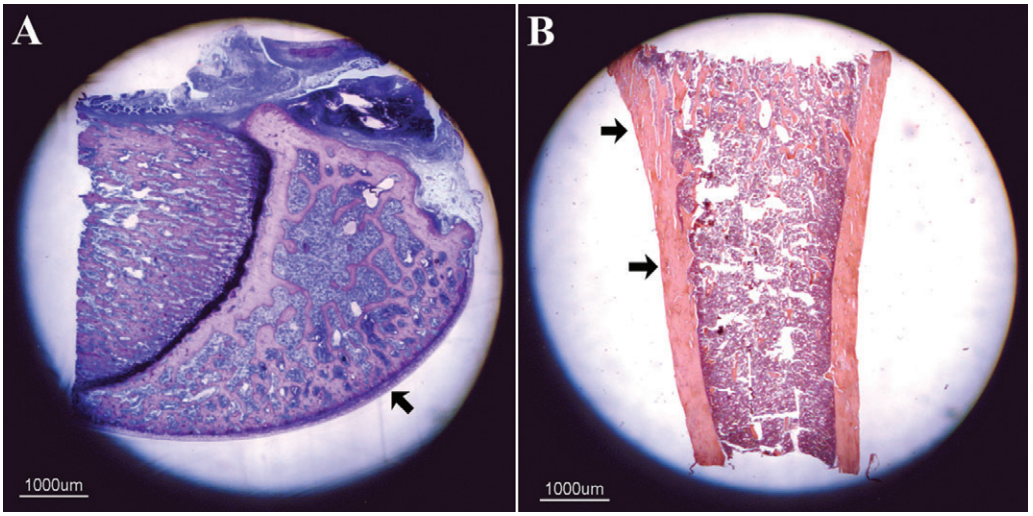

Figure 5 Histological ground and decalcified sections of rat bone. *A*, Ground cross-section of femur epiphysis. *B*, Paraffin-embedded and H&E-stained longitudinal section of rat tibia. The sampling sites are indicated by arrows (magnification ×4). H&E = hematoxylin and eosin.

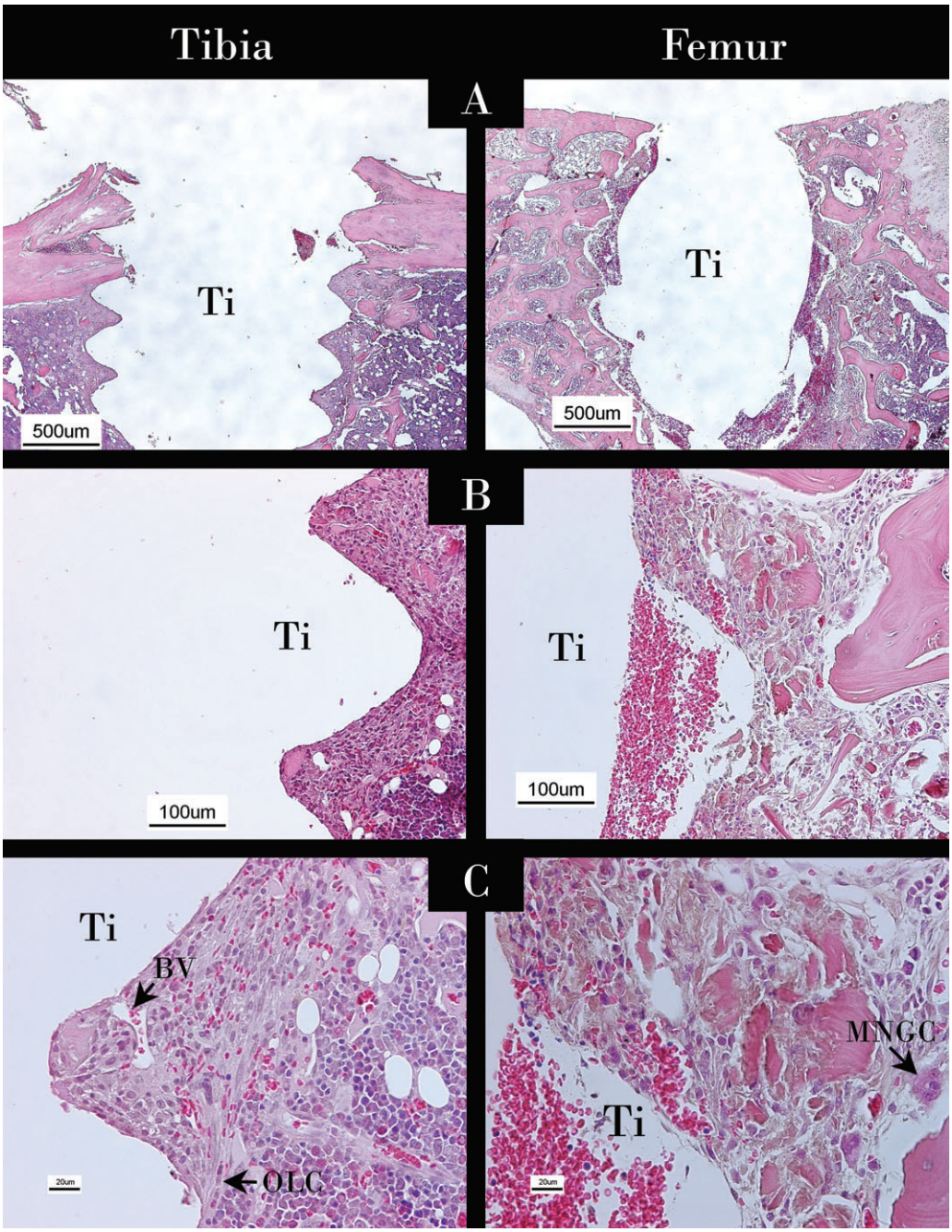

Figure 6 Histological serial decalcified sections of the tissue-implant interface after 3 days of implantation in tibia (left) and femur (right). The implant (Ti) is removed. The lower magnification image (A) (×4 magnification) shows that the bone-implant interface is more preserved and undisrupted in the tibia compared to the femur. The higher magnifications (B and C) (×20 and ×40 magnification, respectively) demonstrate a higher degree of new tissue organization and regeneration at the tibial sites. At the tibial implants, osteoblast-like cells (OLC) and newly formed blood vessels (BV) are detected (some of which are indicated by arrows). The femoral implant site is less well organized. Bone fragments are distributed in the marrow surrounding the implants. Multinuclear giant cells (MNGC) could be recognized close to bone spicules.

regeneration at this early stage of healing. The tissue located inside the threads was well organized (see Figure 6B) and different cellular populations could be distinguished (see Figure 6C).

DISCUSSION

For the first time qPCR was used to explore the differences in relative gene expression between cortical and

trabecular bone types. Higher expression levels of genes denoting bone remodeling were found in the trabecular femoral epiphysis compared with the cortico-trabecular proximal tibial metaphysis and the cortical distal tibial metaphysis (see Figure 1, A and B, Tables 1 and 2). One explanation for the different expression levels between the femur and tibia sites could be the nature of endochondral bone formation taking place at some locations in femur epiphysis (see Figure 4, D–F). Actively mitotic cells in the growth plates and the new matrix formation are consistent with increased levels of ALP and OC as shown in the results. High CATK and TRAP mRNA expression is likely due to the active osteoclastic (chondroclastic) action. Differences in the content of the highly osteoinductive bone morphogenic proteins (BMPs) were described between intramembraneous and endochondral bone types.[17] A recent study[23] showed that the expression of the BMPs BMP-2 and BMP-4 were significantly higher in trabecular than in cortical bone. The difference in the total level of CATK expression between the proximal and distal tibial bone was in line with histological data showing higher bone resorption and bone formation at the proximal tibia site (see Figure 4, B and C). Higher expression levels of IL-1β and TNF-α were observed in both tibia sites compared with the femur. IL-1β and TNF-α are pro-inflammatory cytokines mainly produced by activated macrophages, lymphocytes, and neutrophils.[27] It has been suggested that the level of TNF-α activity is crucial in controlling bone formation, fracture repair, and diseases.[28] However, the exact connection between the pro-inflammatory cytokines production and bone remodelling is not yet understood.

For the first time, the gene expression at titanium implants was compared in the bone beds of cortical and trabecular types. The comparison shows that the two bone types responded differently to the same implant type after 3 days of implantation. Using rabbit femur model, Roberts and colleagues showed that the new bone formation at the implant started already after 3 days of implantation.[29] Further, the response of rabbit tibia to titanium implants after 3 days of implantation was characterized by migration of mesenchymal cells to the implant site and formation of osteoblast seams and osteoid.[30] Recently, differences in gene expression denoting inflammation and bone remodeling were detected as early as after 1 and 3 days, respectively, between different implants in the present rat tibia model.[5] In the current study, the early pro-inflammatory response, represented by IL-1β, was greater in the trabecular bone whereas bone formation activity, represented by ALP and OC, was considerably higher in the cortical bone. The histological observations of the bone-implant interface in the present study (see Figure 6) support the gene expression data in that a higher degree of new tissue regeneration and organization was associated with oxidized implant in the cortical site compared to the trabecular one. In the present study, the gene expression denoting inflammation and bone remodeling activities was reversed from the steady-state expression. If this cannot be explained by the different sampling techniques used which may result in differences in the bone remodeling phase between the samples, it suggests a strong perturbation of bone activity in response to the implanted material. Then it may be assumed that the upregulated pro-inflammatory response in femur potentially interfered with the bone formation process after 3 days of implantation. Such assumption needs to be verified using additional time periods, morphological techniques, and different types of implants.

The available literature on the response of different bone types to implants is contradictory. Whereas some authors have noticed a superior response of trabecular bone over the cortical type,[1–4] others have proved stronger bone formation at implants in cortical bone locations.[31,32] In the current study, we used anodically oxidized titanium implants, which have been shown to have enhanced osteointegration.[33–38] Studies on similar types of implants with and without phosphorylcholine coating showed that the peri-implant bone density, within as well as immediately outside the implant threads, was considerably greater at the tibial cortical sites than at the femoral trabecular sites.[32] On the other hand, Ivanoff and colleagues[39] showed that titanium implants intentionally inserted with poor primary stability in the femoral trabecular bone was associated with more bone in implant threads compared with the stable control implants. Using a similar approach in the cortical bone failed to cause any significant difference between test and stable control implants. The author suggested that trabecular bone might respond more positively to mechanical stimulation than the cortical type. The results of the present study suggest that not only mechanical stimulation can explain the difference between trabecular and cortical bone responses, but

the differences in the pro-inflammatory and remodeling rates shall be considered.

CONCLUSIONS

The present study shows that during steady-state conditions, the bone with trabecular architecture expresses higher level of bone turnover markers compared with the cortical bone, while the later has a higher inflammatory potential. The response to anodically oxidized titanium implants is different in trabecular and cortical bone sites after 3 days of implantation. Such variations should be taken into account when analyzing bone tissue response to injury and for the evaluation of biomaterials. qPCR provides a sensitive technique to discriminate and characterize responses of different bone types to biomaterials using the same model.

ACKNOWLEDGMENTS

We want to thank TATAA Biocenter AB, Göteborg, Sweden, for performing the gene expression analysis. This work was supported by VINNOVA VinnVäxt program Biomedical Development in Western Sweden, the Swedish Research Council (grant K2006-73X09495-16-3), Nobel Biocare AB, Göteborg, Sweden, and the Institute of Biomaterials and Cell Therapy.

REFERENCES

1. Haider R, Watzek G, Plenk H. Effects of drill cooling and bone structure on IMZ implant fixation. Int J Oral Maxillofac Implants 1993; 8:83–91.
2. Davies JE. Understanding peri-implant endosseous healing. J Dent Educ 2003; 67:932–949.
3. Malmstrom J, Adolfsson E, Arvidsson A, Thomsen P. Bone response inside free-form fabricated macroporous hydroxyapatite scaffolds with and without an open microporosity. Clin Implant Dent Relat Res 2007; 9:79–88.
4. Mohammadi S, Esposito M, Hall J, Emanuelsson L, Krozer A, Thomsen P. Short-term bone response to titanium implants coated with thin radiofrequent magnetron-sputtered hydroxyapatite in rabbits. Clin Implant Dent Relat Res 2003; 5:241–253.
5. Omar O, Svensson S, Zoric N, et al. In vivo gene expression in response to anodically oxidized versus machined titanium implants. J Biomed Mater Res A 2009. (In press)
6. Gabbay JS, Heller J, Spoon DB, et al. Noggin underexpression and runx-2 overexpression in a craniosynostosis rabbit model. Ann Plast Surg 2006; 56:306–311.
7. Honsawek S, Powers RM, Wolfinbarger L. Extractable bone morphogenetic protein and correlation with induced new bone formation in an in vivo assay in the athymic mouse model. Cell Tissue Bank 2005; 6:13–23.
8. McKee MD, Farach-Carson MC, Butler WT, Hauschka PV, Nanci A. Ultrastructural immunolocalization of noncollagenous (osteopontin and osteocalcin) and plasma (albumin and alpha 2HS-glycoprotein) proteins in rat bone. J Bone Miner Res 1993; 8:485–496.
9. Pufe T, Scholz-Ahrens KE, Franke AT, et al. The role of vascular endothelial growth factor in glucocorticoid-induced bone loss: evaluation in a minipig model. Bone 2003; 33:869–876.
10. Wildemann B, Kadow-Romacker A, Pruss A, Haas NP, Schmidmaier G. Quantification of growth factors in allogenic bone grafts extracted with three different methods. Cell Tissue Bank 2007; 8:107–114.
11. Zhang J, Lu Y, Dai J, et al. In vivo real-time imaging of TGF-beta-induced transcriptional activation of the RANK ligand gene promoter in intraosseous prostate cancer. Prostate 2004; 59:360–369.
12. Hopwood B, Tsykin A, Findlay DM, Fazzalari NL. Microarray gene expression profiling of osteoarthritic bone suggests altered bone remodelling, WNT and transforming growth factor-beta/bone morphogenic protein signalling. Arthritis Res Ther 2007; 9:R100.
13. Ikeda T, Nagai Y, Yamaguchi A, Yokose S, Yoshiki S. Age-related reduction in bone matrix protein mRNA expression in rat bone tissues: application of histomorphometry to in situ hybridization. Bone 1995; 16:17–23.
14. Kishimoto K, Kitazawa R, Kurosaka M, Maeda S, Kitazawa S. Expression profile of genes related to osteoclastogenesis in mouse growth plate and articular cartilage. Histochem Cell Biol 2006; 125:593–602.
15. Ozawa S, Ogawa T, Iida K, et al. Ovariectomy hinders the early stage of bone-implant integration: histomorphometric, biomechanical, and molecular analyses. Bone 2002; 30:137–143.
16. Schierano G, Canuto RA, Navone R, et al. Biological factors involved in the osseointegration of oral titanium implants with different surfaces: a pilot study in minipigs. J Periodontol 2005; 76:1710–1720.
17. Suttapreyasri S, Koontongkaew S, Phongdara A, Leggat U. Expression of bone morphogenetic proteins in normal human intramembranous and endochondral bones. Int J Oral Maxillofac Surg 2006; 35:444–452.
18. Zhu WQ, Wang X, Wang XX, Wang ZY. [Molecular mechanism of bone remodelling during mandibular distraction osteogenesis in rats.] Zhonghua Kou Qiang Yi Xue Za Zhi 2007; 42:729–732. (In Chinese)
19. Masaki C, Schneider GB, Zaharias R, Seabold D, Stanford C. Effects of implant surface microtopography on osteoblast gene expression. Clin Oral Implants Res 2005; 16:650–656.
20. Schneider GB, Zaharias R, Seabold D, Keller J, Stanford C. Differentiation of preosteoblasts is affected by implant

surface microtopographies. J Biomed Mater Res A 2004; 69:462–468.
21. Tan KS, Qian L, Rosado R, Flood PM, Cooper LF. The role of titanium surface topography on J774A.1 macrophage inflammatory cytokines and nitric oxide production. Biomaterials 2006; 27:5170–5177.
22. Guo J, Padilla RJ, Ambrose W, De Kok IJ, Cooper LF. The effect of hydrofluoric acid treatment of TiO2 grit blasted titanium implants on adherent osteoblast gene expression in vitro and in vivo. Biomaterials 2007; 28:5418–5425.
23. Kochanowska I, Chaberek S, Wojtowicz A, et al. Expression of genes for bone morphogenetic proteins BMP-2, BMP-4 and BMP-6 in various parts of the human skeleton. BMC Musculoskelet Disord 2007; 8:128.
24. Preti G, Martinasso G, Peirone B, et al. Cytokines and growth factors involved in the osseointegration of oral titanium implants positioned using piezoelectric bone surgery versus a drill technique: a pilot study in minipigs. J Periodontol 2007; 78:716–722.
25. Rozen S, Skaletsky H. Primer3 on the WWW for general users and for biologist programmers. Methods Mol Biol 2000; 132:365–386.
26. Pfaffl MW. A new mathematical model for relative quantification in real-time RT-PCR. Nucleic Acids Res 2001; 29:e45.
27. Lo YJ, Liu CM, Wong MY, Hou LT, Chang WK. Interleukin 1beta-secreting cells in inflamed gingival tissue of adult periodontitis patients. Cytokine 1999; 11:626–633.
28. Zhou FH, Foster BK, Zhou XF, Cowin AJ, Xian CJ. TNF-alpha mediates p38 MAP kinase activation and negatively regulates bone formation at the injured growth plate in rats. J Bone Miner Res 2006; 21:1075–1088.
29. Roberts WE, Smith RK, Zilberman Y, Mozsary PG, Smith RS. Osseous adaptation to continuous loading of rigid endosseous implants. Am J Orthod 1984; 86:95–111.
30. Sennerby L, Thomsen P, Ericson LE. Early tissue response to titanium implants inserted in rabbit cortical bone: part I light microscopic observations. J Mater Sci Mater Med 1993; 4:240–250.
31. Lu JX, Gallur A, Flautre B, et al. Comparative study of tissue reactions to calcium phosphate ceramics among cancellous, cortical, and medullar bone sites in rabbits. J Biomed Mater Res 1998; 42:357–367.
32. Susin C, Qahash M, Hall J, Sennerby L, Wikesjo UM. Histological and biomechanical evaluation of phosphorylcholine-coated titanium implants. J Clin Periodontol 2008; 35:270–275.
33. Albrektsson T, Johansson C, Lundgren A-K, Sul Y-T, Gottlow J. Experimental studies on oxidized implants. A histomorphometrical and biomechanical analysis. Appl Osseointegration Res 2000; 1:21–24.
34. Gottlow J, Johansson C, Albrektsson T, Lundgren A-K. Biomechanical and histologic evaluation of the TiUnite and Osseotite implant surfaces in rabbits after 6 weeks of healing. Appl Osseointegration Res 2000; 1:25–30.
35. Rocci A, Martignoni M, Gottlow J. Immediate loading of Branemark System TiUnite and machined-surface implants in the posterior mandible: a randomized open-ended clinical trial. Clin Implant Dent Relat Res 2003; 5(Suppl 1):57–63.
36. Schupbach P, Glauser R, Rocci A, et al. The human bone-oxidized titanium implant interface: a light microscopic, scanning electron microscopic, back-scatter scanning electron microscopic, and energy-dispersive x-ray study of clinically retrieved dental implants. Clin Implant Dent Relat Res 2005; 7(Suppl 1):S36–S43.
37. Sul YT, Johansson C, Albrektsson T. Which surface properties enhance bone response to implants? Comparison of oxidized magnesium, TiUnite, and Osseotite implant surfaces. Int J Prosthodont 2006; 19:319–328.
38. Zechner W, Tangl S, Furst G, et al. Osseous healing characteristics of three different implant types. Clin Oral Implants Res 2003; 14:150–157.
39. Ivanoff CJ, Sennerby L, Lekholm U. Influence of initial implant mobility on the integration of titanium implants. An experimental study in rabbits. Clin Oral Implants Res 1996; 7:120–127.